Journal of Zhejiang University-SCIENCE B (Biomedicine & Biotechnology) 2023 24(3):275-280
www.jzus.zju.edu.cn; www.springer.com/journal/11585
E-mail: jzus_b@zju.edu.cn

## Correspondence

https://doi.org/10.1631/jzus.B2200622

# An epipolythiodioxopiperazine alkaloid and diversified aromatic polyketides with cytotoxicity from the Beibu Gulf coral-derived fungus *Emericella nidulans* GXIMD 02509

Miaoping LIN*, Zhenzhou TANG*, Jiaxi WANG, Humu LU, Chenwei WANG, Yanting ZHANG, Xinming LIU, Chenghai GAO, Yonghong LIU, Xiaowei LUO✉

*Institute of Marine Drugs, Guangxi Key Laboratory of Marine Drugs, Guangxi University of Chinese Medicine, Nanning 530200, China*

Marine microorganisms, especially marine fungi, have historically proven their value as a prolific source for structurally novel and pharmacologically active secondary metabolites (Deshmukh et al., 2018; Carroll et al., 2022). The corals constitute a dominant part of reefs with the highest biodiversity, and harbor highly diverse and abundant microbial symbionts in their tissue, skeleton, and mucus layer, with species-specific core members that are spatially partitioned across coral microhabitats (Wang WQ et al., 2022). The coral-associated fungi were very recently found to be vital producers of structurally diverse compounds, terpenes, alkaloids, peptides, aromatics, lactones, and steroids. They demonstrate a wide range of bioactivity such as anticancer, antimicrobial, and antifouling activity (Chen et al., 2022). The genetically powerful genus *Emericella* (Ascomycota), which has marine and terrestrial sources, includes over 30 species and is distributed worldwide. It is considered a rich source of diverse secondary metabolites with antimicrobial activity or cytotoxicity (Alburae et al., 2020). Notably, *Emericella nidulans*, the sexual state of a classic biosynthetic strain *Aspergillus nidulans*, was recently reported as an important source of highly methylated polyketides (Li et al., 2019) and isoindolone-containing meroterpenoids (Zhou et al., 2016) with unusual skeletons.

The Beibu Gulf is a semi-enclosed gulf in the northwest of the South China Sea, and harbors tremendous underexplored biodiversity in terms of both marine organisms and microorganisms; these are rich in diversified secondary metabolites (Huang et al., 2022). In continuation of our efforts to discover interesting lead compounds from Beibu Gulf coral-derived marine fungi, a plethora of structurally novel secondary metabolites with remarkable biological activity have been recently obtained, including anti-tumor ascochlorins (Guo et al., 2021; Luo et al., 2021) and cytochalasans (Luo et al., 2020), anti-osteoclastogenic chlorinated polyketides (Zhang et al., 2022), phenolic derivatives (Lu et al., 2022), and cyclopiazonic acid alkaloids (Wang JM et al., 2022). In this study, a fungus *Emericella nidulans* GXIMD 02509 endemic to Weizhou coral reefs attracted our attention owing to the intriguing high-performance liquid chromatography (HPLC)-ultraviolet (UV) profiles of its extract. Subsequent chemical investigation led to the isolation of nine diverse aromatic polyketides, an epipolythiodioxopiperazine alkaloid, and a farnesylated phthalide derivative (Fig. 1). Several of these compounds showed cytotoxicity against three human cancer-cell lines (786-O, SW1990, and SW480). Here, the process of isolation and structural determination, as well as the cytotoxicity results, are described in detail.

Compound **1** was isolated as a bright-yellow solid and was deduced with the molecular formula $C_{21}H_{22}O_6$ based on the high resolution-electrospray ionization-mass spectroscopy (HR-ESI-MS) data $[M+H]^+$ ion peak at *m/z* 371.1499 (calcd for $C_{21}H_{23}O_6$, 371.1495). The UV spectrum revealed the presence of benzene chromophores with absorption bands at 203, 255, and 320 nm. The $^1H$ nuclear magnetic resonance (NMR) (Table 1) and heteronuclear single quantum coherence

✉ Xiaowei LUO, luoxiaowei1991@126.com
* The two authors contributed equally to this work
Xiaowei LUO, https://orcid.org/0000-0002-2114-1609

Received Dec. 7, 2022; Revision accepted Jan. 6, 2023; Crosschecked Feb. 17, 2023

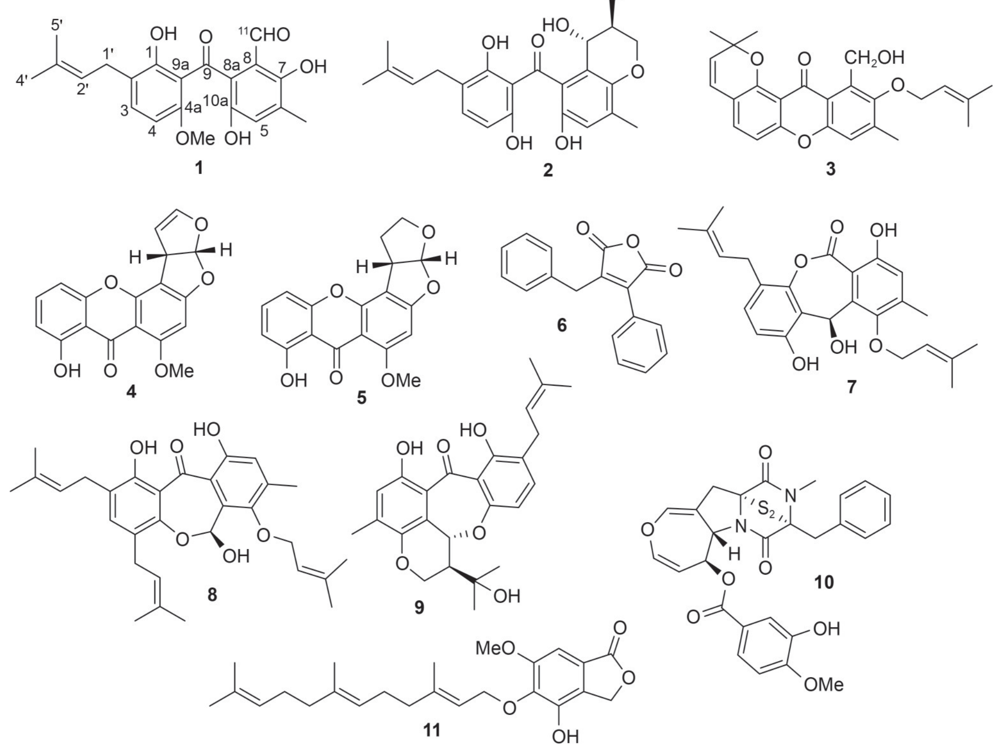

**Fig. 1 Chemical structures of compounds 1–11.**

(HSQC) data for **1** displayed a series of signals, including: two hydroxyl groups attributable to 1-OH ($\delta_H$ 10.93, s) and 7-OH ($\delta_H$ 11.38, s); one aldehyde group, H-11 ($\delta_H$ 9.98, s); four aromatic or olefinic protons, H-3 ($\delta_H$ 7.12, d, *J*=8.5 Hz), H-4 ($\delta_H$ 6.12, d, *J*=8.5 Hz), H-5 ($\delta_H$ 7.16, s), and H-2' ($\delta_H$ 5.25, t, *J*=7.0 Hz); one methylene, H-1' ($\delta_H$ 3.28, d, *J*=7.0 Hz); three singlet methyls, 6-Me ($\delta_H$ 2.24, s), $H_3$-4' ($\delta_H$ 1.72, s), and $H_3$-5' ($\delta_H$ 2.24, s); and one methoxyl, 4a-OMe ($\delta_H$ 4.03, s). Aside from these ten corresponding hydrogen-bearing carbons, ten aromatic or olefinic (four oxygenated) carbons and a carbonyl ($\delta_C$ 198.3) remained in the $^{13}$C NMR spectrum.

This information revealed that structurally, **1** was closely related to arugosin H, which was also obtained from the marine-derived fungus *Emericella nidulans* var. *acristata* (Kralj et al., 2006). The main difference was the appearance of a methoxyl group ($\delta_{H/C}$ 4.03/53.2) at C-4a ($\delta_C$ 170.5) in **1** instead of the hydroxyl group that appears in arugosin H. This deduction was verified by the heteronuclear multiple bond correlation (HMBC) correlation from 4a-OC$\underline{H}_3$ to C-4a (Fig. 2). Based on these findings, we determined that the structure of **1** was a methyl derivative of arugosin H, and accordingly assigned it a trival name: 4a-*O*-methoxyarugosin H (Figs. S1–S9). Compound **1** was probably an artifact produced during the isolation procedure when methanol was used as the main solvent (Capon, 2020).

We were able to pinpoint known compounds by comparing the physicochemical data of known compounds **2**–**11** (supplementary information) with data from the literature. We identified pre-shamixanthone (**2**) (Wu et al., 2015a), cycloisoemericellin (**3**) (Kawahara et al., 1988), sterigmatocystin (**4**) (Zhu and Lin, 2007), dihydrosterigmatocystin (**5**) (Zhu and Lin, 2007), dehydromicroperfuranone (**6**) (Kralj et al., 2006; Roux et al., 2020), varioxiranol I (**7**) (Wu et al., 2015b), arugosin G (**8**) (Kralj et al., 2006), arugosin C (**9**) (Kawahara et al., 1988; El-Kashef et al., 2021), emestrin J (**10**) (Li et al., 2016), and farnesylemefuranone D (**11**) (Chi et al., 2020). Interestingly, emestrin J (**10**) harbors with an uncommon disulfide moiety, which was biosynthesized by a peptide cyclization pathway along with additional ring-expansion and macrocyclization (Li et al., 2016).

During the course of our search for anti-tumor lead compounds from marine natural products (Zhou

**Table 1  $^1$H (500 MHz) and $^{13}$C (125 MHz) NMR spectroscopic data for 4a-*O*-methoxyarugosin H (1) ($CDCl_3$)**

| Position | $\delta_C$, type | $\delta_H$ ($J$ (Hz)) | HMBC |
|---|---|---|---|
| 1 | 160.4, C | | |
| 2 | 125.2, C | | |
| 3 | 134.9, CH | 7.12, d (8.5) | 1, 1' |
| 4 | 105.5, CH | 6.12, d (8.5) | 2, 4a, 9a |
| 4a | 170.5, C | | |
| 4a-OMe | 53.2, $CH_3$ | 4.03, s | 4a |
| 5 | 128.0, CH | 7.16, s | 6, 6-Me, 7, 10a |
| 6 | 139.8, C | | |
| 6-Me | 15.2, $CH_3$ | 2.24, s | 5, 6, 7 |
| 7 | 154.8, C | | |
| 8 | 113.7, C | | |
| 8a | 125.3, C | | |
| 9 | 198.3, C | | |
| 9a | 103.5, C | | |
| 10a | 140.2, C | | |
| 11 | 194.1, CH | 9.98, s | 7, 8, 8a |
| 1' | 27.8, $CH_2$ | 3.28, d (7.0) | 1, 2, 3, 2', 3' |
| 2' | 121.5, CH | 5.25, t (7.0) | 2, 1', 4', 5' |
| 3' | 133.7, C | | |
| 4' | 25.9, $CH_3$ | 1.72, s | 2', 3', 5' |
| 5' | 17.9, $CH_3$ | 2.24, s | 2', 3', 4' |
| 1-OH | | 10.93, s | 1, 2, 9a |
| 7-OH | | 11.38, s | 6, 7, 8 |

NMR: nuclear magnetic resonance; HMBC: heteronuclear multiple bond correlation.

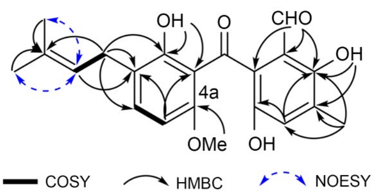


**Fig. 2  Key $^1$H-$^1$H COSY, HMBC, and NOESY correlations of 4a-*O*-methoxyarugosin H (1). COSY: correlation spectroscopy; HMBC: heteronuclear multiple bond correlation; NOESY: nuclear overhauser effect spectroscopy.**

et al., 2019; Luo et al., 2021), all obtained compounds were evaluated for cytotoxicity against three human cancer cell lines, i.e., 786-O (human renal carcinoma cell), SW1990 (human pancreatic cancer cell), and SW480 (human colorectal cancer cell), along with the normal human liver cell line LO2 (Table 2). Among them, compounds **1**–**5**, **7**, and **10** showed inhibitory activity against these cell lines, with the half maximal inhibitory concentration ($IC_{50}$) values ranging from 4.3 to 33.4 μmol/L. Notably, emestrin J (**10**) exhibited the strongest activity against these cancer cell lines,

**Table 2  Cytotoxicity of compounds 1–11**

| Compound | $IC_{50}$ (μmol/L) | | | |
|---|---|---|---|---|
| | 786-O | SW1990 | SW480 | LO2 |
| **1** | – | – | 32.6±1.2 | – |
| **2** | – | 33.2±5.1 | – | – |
| **3** | – | 24.7±2.2 | 30.2±4.8 | – |
| **4** | 18.3±1.9 | 19.6±2.8 | – | – |
| **5** | 24.7±1.8 | – | – | – |
| **6** | – | – | – | – |
| **7** | 33.4±1.8 | 30.4±5.1 | 27.2±6.5 | – |
| **8** | – | – | – | – |
| **9** | – | – | – | – |
| **10** | 4.3±0.7 | 14.1±1.8 | 4.9±0.3 | 11.1±2.4 |
| **11** | – | – | – | – |
| Cisplatin | 2.5±0.6 | 33.8±4.7 | 26.7±4.6 | 5.2±0.6 |

All data shown above are mean±SD of three independent experiments. $IC_{50}$: half maximal inhibitory concentration; SD: standard deviation. "–": >40 μmol/L.

especially for 786-O (4.3 μmol/L), and was at least as potent as the positive control, cisplatin. Interestingly, two xanthone derivatives (**4** and **5**) displayed antiproliferative activity, with $IC_{50}$ values of 18.3 and 24.7 μmol/L against 786-O, and 19.6 and >40 μmol/L against SW1990 cells, respectively. This revealed that the $\Delta^{16}$ double bond in **4** probably promoted cytotoxic activity.

To further evaluate the potential anti-tumor activity of **10**, we next investigated its activity against 786-O cells in cell colony and scratch wound assays. Consistent with the above-mentioned antiproliferative activity, compound **10** significantly reduced cell colony formation of 786-O cells at concentrations of 0.5 and 1.0 μmol/L (Figs. 3a and 3b). Also, compared with the vehicle group, compound **10** significantly suppressed migration of 786-O cells in a time- and dose-dependent manner (Figs. 3c and 3d). To explore whether the antiproliferative activity of **10** was related to apoptosis, we further evaluated the compound for its effect on cell apoptosis and cell-cycle arrest in 786-O cells. The results were analyzed by flow cytometry and showed that the total apoptotic cells (early and late) induced by **10** at 24 h rose by 21.4% (2 μmol/L) and 29.5% (4 μmol/L), suggesting that **10** induced 786-O cell apoptosis in a dose-dependent manner (Figs. 4a and 4b). Meanwhile, the cell-cycle distribution results revealed that **10** primarily blocked the cell cycle during the G2/M phase, resulting in an inability of cells to proliferate (Figs. 4c and 4d). Therefore, it was clear that **10** could suppress the proliferation, colony formation, and

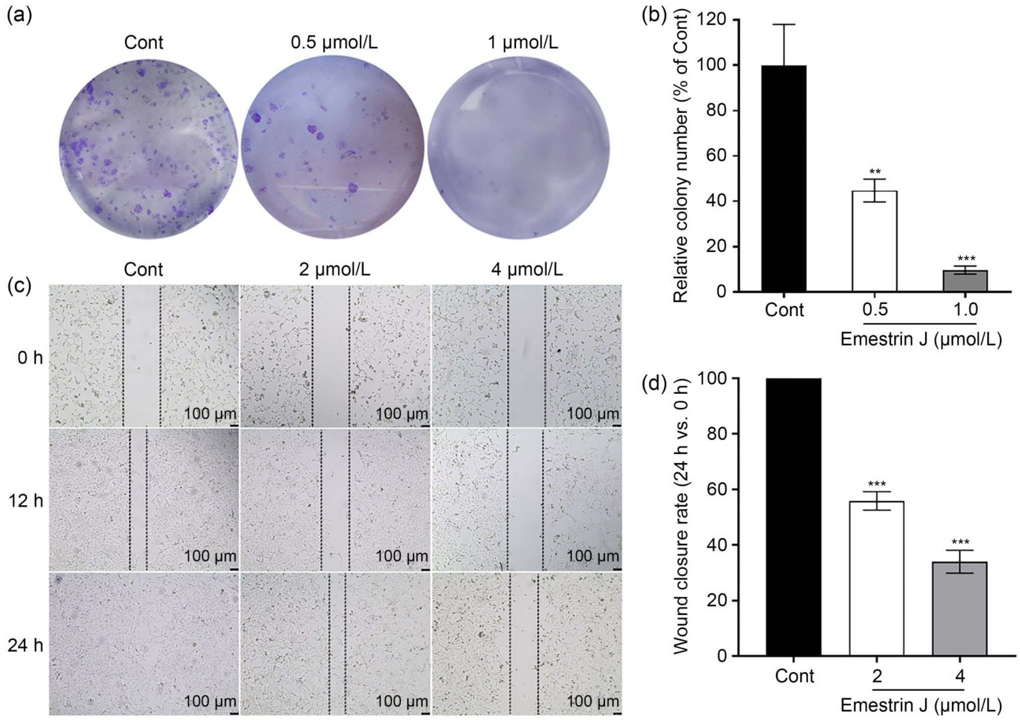


**Fig. 3 Suppressive effects of emestrin J (10) on colony formation and migration of 786-O cells in vitro. Representative wells (a) and quantitative results (b) of the colony-formation assay. Representative images (c) and quantitative results (d) of the scratch wound assay. 786-O cells were treated with vehicle (DMSO, Cont) or 10, as indicated. All data shown above are mean±SD of three independent experiments. ** *P*<0.01, *** *P*<0.001 vs. Cont. DMSO: dimethylsulfoxide; Cont: control; SD: standard deviation.**

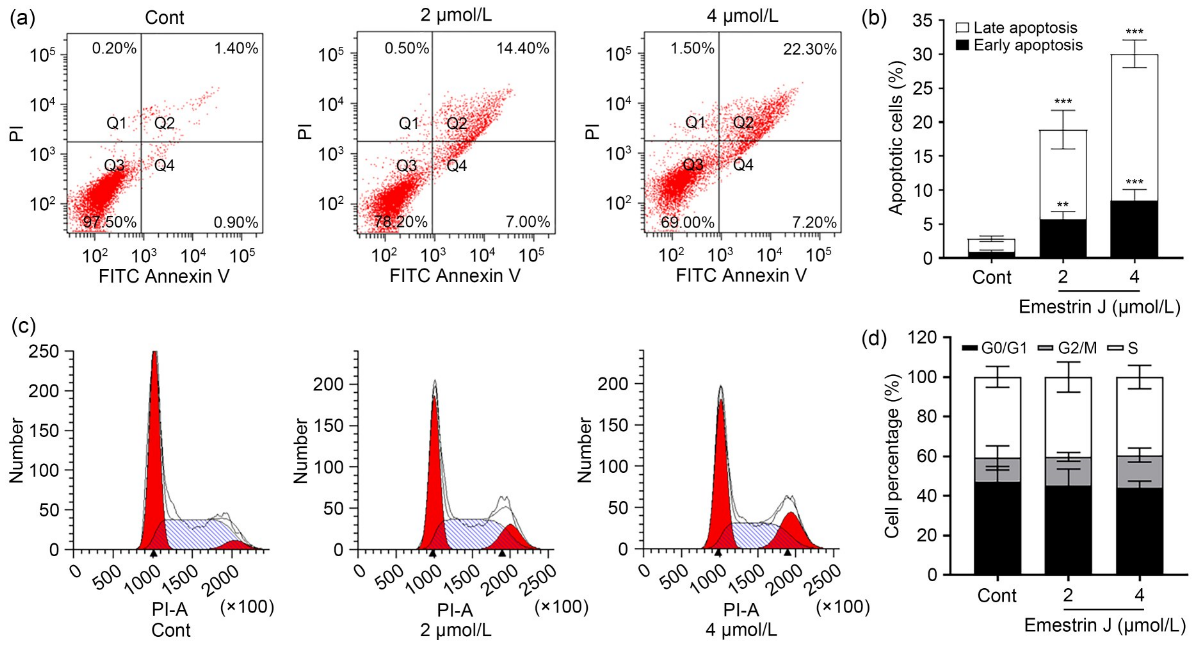


**Fig. 4 Effects of emestrin J (10) on cell apoptosis and cell-cycle arrest in 786-O cells. Emestrin J (10) induced apoptosis of 786-O cells (a, b) and arrested the cell cycle (c, d) in the G2/M phase. 786-O cells were treated with vehicle (DMSO, Cont) or 10 (2 and 4 μmol/L) for 24 h, as indicated. All data shown above are mean±SD of three independent experiments. ** *P*<0.01, *** *P*<0.001 vs. Cont. DMSO: dimethylsulfoxide; Cont: control; SD: standard deviation; FITC: fluorescein isothiocyanate; PI: propidium iodide; PI-A: PI-area.**

migration of 786-O cells, and induce apoptosis, acting as a potential anti-tumor compound.

In conclusion, nine aromatic polyketides, including a new one, 4a-*O*-methoxyarugosin H (**1**), along with an epipolythiodioxopiperazine alkaloid, emestrin J (**10**), and a farnesylated phthalide derivative, were obtained from the Beibu Gulf coral-associated fungus *Emericella nidulans* GXIMD 02509. We determined their structures by spectral data analysis, as well as comparison with reported data. Several of the compounds exhibit cytotoxicity against three human cancer cell lines, 786-O, SW1990, and SW480. The most potent one, emestrin J (**10**), has an uncommon disulfide bond and suppresses proliferation, colony formation, and migration of 786-O cells, as well as inducing apoptosis. Our findings provide a basis for further development and utilization of emestrin derivatives as sources of potential anti-tumor chemotherapy agents.

## Materials and methods

Detailed methods are provided in the electronic supplementary materials of this paper.

## Acknowledgments

This research was supported by the Guangxi Natural Science Foundation (Nos. 2020GXNSFBA159001, 2020GXNSFGA297002, and 2021GXNSFAA220052), the National Natural Science Foundation of China (Nos. U20A20101 and 22007019), the Special Fund for Bagui Scholars of Guangxi (Yonghong LIU), and the Scientific Research Foundation of Guangxi University of Chinese Medicine (No. 2022C038), China.

## Author contributions

Xiaowei LUO and Yonghong LIU conceived the research and designed experiments. Miaoping LIN, Zhenzhou TANG, Jiaxi WANG, Humu LU, Chenwei WANG, Yanting ZHANG, Xinming LIU, and Chenghai GAO performed the experiments and analysis. Xiaowei LUO, Miaoping LIN, and Zhenzhou TANG interpreted the data and wrote the paper. All authors have read and approved the final manuscript, and therefore, have full access to all the data in the study and take responsibility for the integrity and security of the data.

## Compliance with ethics guidelines

Miaoping LIN, Zhenzhou TANG, Jiaxi WANG, Humu LU, Chenwei WANG, Yanting ZHANG, Xinming LIU, Chenghai GAO, Yonghong LIU, and Xiaowei LUO declare that they have no conflict of interest.

This article does not contain any studies with human or animal subjects performed by any of the authors.

## References

Alburae NA, Mohammed AE, Alorfi HS, et al., 2020. Nidulantes of *Aspergillus* (formerly *Emericella*): a treasure trove of chemical diversity and biological activities. *Metabolites*, 10(2):73. https://doi.org/10.3390/metabo10020073

Capon RJ, 2020. Extracting value: mechanistic insights into the formation of natural product artifacts–case studies in marine natural products. *Nat Prod Rep*, 37(1):55-79. https://doi.org/10.1039/C9NP00013E

Carroll AR, Copp BR, Davis RA, et al., 2022. Marine natural products. *Nat Prod Rep*, 39(6):1122-1171. https://doi.org/10.1039/D1NP00076D

Chen Y, Pang XY, He YC, et al., 2022. Secondary metabolites from coral-associated fungi: source, chemistry and bioactivities. *J Fungi*, 8(10):1043. https://doi.org/10.3390/jof8101043

Chi LP, Li XM, Wan YP, et al., 2020. Ophiobolin sesterterpenoids and farnesylated phthalide derivatives from the deep sea cold-seep-derived fungus *Aspergillus insuetus* SD-512. *J Nat Prod*, 83(12):3652-3660. https://doi.org/10.1021/acs.jnatprod.0c00860

Deshmukh SK, Gupta MK, Prakash V, et al., 2018. Mangrove-associated fungi: a novel source of potential anticancer compounds. *J Fungi*, 4(3):101. https://doi.org/10.3390/jof4030101

El-Kashef DH, Youssef FS, Reimche I, et al., 2021. Polyketides from the marine-derived fungus *Aspergillus falconensis*: *in silico* and *in vitro* cytotoxicity studies. *Bioorg Med Chem*, 29:115883. https://doi.org/10.1016/j.bmc.2020.115883

Guo L, Luo XW, Yang P, et al., 2021. Ilicicolin A exerts antitumor effect in castration-resistant prostate cancer via suppressing EZH2 signaling pathway. *Front Pharmacol*, 12:723729. https://doi.org/10.3389/fphar.2021.723729

Huang BY, Peng S, Liu SF, et al., 2022. Isolation, screening, and active metabolites identification of anti-*Vibrio* fungal strains derived from the Beibu Gulf coral. *Front Microbiol*, 13:930981. https://doi.org/10.3389/fmicb.2022.930981

Kawahara N, Nozawa K, Nakajima S, et al., 1988. Studies on fungal products. Part 15. Isolation and structure determination of arugosin E from *Aspergillus silvaticus* and cycloisoemericellin from *Emericella striata*. *J Chem Soc Perkin Trans*, 1(4):907-911. https://doi.org/10.1039/P19880000907

Kralj A, Kehraus S, Krick A, et al., 2006. Arugosins G and H: prenylated polyketides from the marine-derived fungus *Emericella nidulans* var. *acristata*. *J Nat Prod*, 69(7):995-1000. https://doi.org/10.1021/np050454f

Li Q, Chen CM, He Y, et al., 2019. Emeriones A–C: three highly methylated polyketides with bicyclo[4.2.0]octene and 3,6-dioxabicyclo[3.1.0]hexane functionalities from *Emericella nidulans*. *Org Lett*, 21(13):5091-5095.

https://doi.org/10.1021/acs.orglett.9b01680

Li Y, Yue Q, Krausert NM, et al., 2016. Emestrins: anti-*cryptococcus* epipolythiodioxopiperazines from *Podospora australis*. *J Nat Prod*, 79(9):2357-2363. https://doi.org/10.1021/acs.jnatprod.6b00498

Lu HM, Tan YH, Zhang YT, et al., 2022. Osteoclastogenesis inhibitory phenolic derivatives produced by the Beibu Gulf coral-associated fungus *Acremonium sclerotigenum* GXIMD 02501. *Fitoterapia*, 159:105201. https://doi.org/10.1016/j.fitote.2022.105201

Luo XW, Gao CH, Lu HM, et al., 2020. HPLC-DAD-guided isolation of diversified chaetoglobosins from the coral-associated fungus *Chaetomium globosum* C2F17. *Molecules*, 25(5):1237. https://doi.org/10.3390/molecules25051237

Luo XW, Cai GD, Guo YF, et al., 2021. Exploring marine-derived ascochlorins as novel human dihydroorotate dehydrogenase inhibitors for treatment of triple-negative breast cancer. J Med Chem, 64(18):13918-13932. https://doi.org/10.1021/acs.jmedchem.1c01402

Roux I, Woodcraft C, Hu JY, et al., 2020. CRISPR-mediated activation of biosynthetic gene clusters for bioactive molecule discovery in filamentous fungi. *ACS Synth Biol*, 9(7): 1843-1854. https://doi.org/10.1021/acssynbio.0c00197

Wang JM, Li ZC, Zhang YT, et al., 2022. A new α-cyclopiazonic acid alkaloid identified from the Weizhou Island coral-derived fungus *Aspergillus flavus* GXIMD 02503. *J Ocean Univ China*, 21(5):1307-1312. https://doi.org/10.1007/s11802-022-4959-5

Wang WQ, Tang KH, Wang PX, et al., 2022. The coral pathogen *Vibrio coralliilyticus* kills non-pathogenic holobiont competitors by triggering prophage induction. *Nat Ecol Evol*, 6(8):1132-1144. https://doi.org/10.1038/s41559-022-01795-y

Wu Q, Wu CM, Long HL, et al., 2015a. Varioxiranols A–G and 19-*O*-methyl-22-methoxypre-shamixanthone, PKS and hybrid PKS-derived metabolites from a sponge-associated *Emericella variecolor* fungus. *J Nat Prod*, 78(10):2461-2470. https://doi.org/10.1021/acs.jnatprod.5b00578

Wu Q, Long HL, Liu D, et al., 2015b. Varioxiranols I–L, new lactones from a sponge-associated *Emericella variecolor* fungus. *J Asian Nat Prod Res*, 17(12):1137-1145. https://doi.org/10.1080/10286020.2015.1119127

Zhang YT, Li ZC, Huang BY, et al., 2022. Anti-osteoclastogenic and antibacterial effects of chlorinated polyketides from the Beibu Gulf coral-derived fungus *Aspergillus unguis* GXIMD 02505. *Mar Drugs*, 20(3):178. https://doi.org/10.3390/md20030178

Zhou HB, Sun XH, Li N, et al., 2016. Isoindolone-containing meroperpenoids from the endophytic fungus *Emericella nidulans* HDN12-249. *Org Lett*, 18(18):4670-4673. https://doi.org/10.1021/acs.orglett.6b02297

Zhou XF, Liang Z, Li KL, et al., 2019. Exploring the natural piericidins as anti-renal cell carcinoma agents targeting peroxiredoxin 1. *J Med Chem*, 62(15):7058-7069. https://doi.org/10.1021/acs.jmedchem.9b00598

Zhu F, Lin YC, 2007. Three xanthones from a marine-derived mangrove endophytic fungus. *Chem Nat Compd*, 43(2):132-135. https://doi.org/10.1007/s10600-007-0062-9

**Supplementary information**

Materials and methods; Figs. S1–S9; Physicochemical data of known compounds **2–11**